

Geometric Variability of the Scoliotic Spine Using Statistics on Articulated Shape Models

Jonathan Boisvert, Farida Cheriet, Xavier Pennec, Hubert Labelle, Nicholas Ayache

Abstract—This paper introduces a method to analyze the variability of the spine shape and of the spine shape deformations using articulated shape models. The spine shape was expressed as a vector of relative poses between local coordinate systems of neighbouring vertebrae. Spine shape deformations were then modeled by a vector of rigid transformations that transforms one spine shape into another. Because rigid transforms do not naturally belong to a vector space, conventional mean and covariance could not be applied. The Fréchet mean and a generalized covariance were used instead. The spine shapes of a group of 295 scoliotic patients were quantitatively analyzed as well as the spine shape deformations associated with the Cotrel-Dubousset corrective surgery (33 patients), the Boston brace (39 patients) and the scoliosis progression without treatment (26 patients). The variability of inter-vertebral poses was found to be inhomogeneous (lumbar vertebrae were more variable than the thoracic ones) and anisotropic (with maximal rotational variability around the coronal axis and maximal translational variability along the axial direction). Finally, brace and surgery were found to have a significant effect on the Fréchet mean and on the generalized covariance in specific spine regions where treatments modified the spine shape.

Index Terms—Statistical Shape Analysis, Anatomical Variability, Rigid Transforms, Spine, Radiograph, Orthopaedic Treatment, Scoliosis

I. INTRODUCTION

Adolescent idiopathic scoliosis is a disease that causes a three dimensional deformation of the spine. As suggested by its name, the cause of the pathology remains unknown. Furthermore, the shape of a scoliotic spine varies greatly from a patient to another. Previous statistical studies (such as [1]–[4]) investigated the outcome of different treatments in term of the variation of clinical indices used by physicians to quantify the severity of the deformation. However, the variability of the spine geometry was not extensively studied. Two important reasons explain the limited number of studies interested in the geometric variability of the scoliotic spine: the availability of significant data and the lack of statistical tools

Copyright (c) 2007 IEEE. Personal use of this material is permitted. However, permission to use this material for any other purposes must be obtained from the IEEE by sending a request to pubs-permissions@ieee.org. Manuscript received August 15, 2006; revised March 25, 2007.

Jonathan Boisvert and Farida Cheriet are affiliated with the École Polytechnique de Montréal, Montréal, Canada.

Jonathan Boisvert, Xavier Pennec and Nicholas Ayache are affiliated with the INRIA, Sophia-Antipolis Cedex, France.

Jonathan Boisvert, Farida Cheriet and Hubert Labelle are affiliated with the Sainte-Justine Hospital, Montréal, Canada.

This work was funded by the Natural Sciences and Engineering Research Council (NSERC) of Canada, the Quebec’s Technology and Nature Research Funds (Fonds de Recherche sur la Nature et les Technologies du Québec) and the Canadian Institutes of Health Research (CIHR).

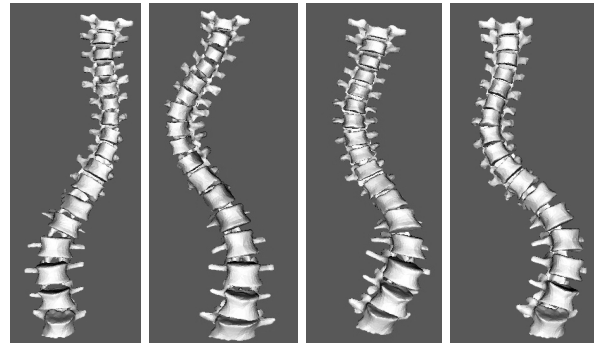


Fig. 1. Some examples of scoliotic spine shapes from our patient database

to handle geometric primitives that are not naturally embedded in vector spaces. In the past, the vast majority of the studies analyzed the geometry of the spine using indices derived from the patient’s radiographs or from 3D reconstructions of his/her spine. Those indices were used to classify the spines’ curves [5]–[8] and also to compare the outcome of different orthopaedic treatments [1]–[4], [9]. The most popular index is certainly the Cobb angle [10], but there are several other indices such as the orientation of the plane of maximal deformity or the spine torsion [11]. Those indices have the advantage of enabling physicians to assess quickly and easily the severity of the scoliosis. However, they also present many problems. First of all, most clinical indices are global to the whole spine and thus do not provide spatial insight about the local geometry. Furthermore, most of the indices (including the Cobb angle) are computed on 2D projections, where a significant part of the curvature could be hidden (since the deformity is three-dimensional).

To overcome those limitations, some authors investigated the scoliotic spine geometry or the effect of orthopaedic treatments by measuring the position and orientation of vertebrae. Those descriptors provide insights that are both local and geometric. Ghanem et al. [12] proposed a method to compute vertebrae translation and orientation during a surgery using an opto-electronic device. Unfortunately, it was a preliminary study and measures were only performed on a group of eight patients. Furthermore, translation and orientation were computed just for the vertebrae adjacent to the apex of the curvature.

Sawatzky et al. [13] performed a similar study, but their goal was to find a relation between the number of hooks installed during a corrective surgery and the position and orientation of the vertebrae. This study was performed on a larger group of patients (32), which allowed the computation

of more advanced statistics. However, only the results for the apical vertebra were reported in their article.

More recently, Petit et al. [14] compared inter-vertebral displacements in term of modifications of the center of rotation for two types of instrumentation used during corrective surgeries (Colorado and Cotrel-Dubousset). The patient sample used was larger than for previously cited studies (82 patients), which made statistically significant more subtle differences between the two groups of patients. Furthermore, results for all vertebrae were reported (not only vertebrae adjacent to the curve apex). However, the authors did not study extensively the variability of the displacement of the center of rotation or of the vertebrae rotations.

One of the common limitations of those studies is that only mean values of the modifications of the positions or of the orientations of the vertebrae were extensively studied. An analysis of the mean spine shape using both orientations and positions of the vertebrae was never published. Furthermore, the variability of the spine anatomy was not studied in that context either.

Unlike surgical treatments, braces effects were never analysed using the relative positions and orientations of the vertebrae. Usually, braces effects were analyzed primarily by measuring the Cobb angle (which is only a two-dimensional measure) of the major curve in the frontal plane [15], [16]. Some studies tried to take into account the three-dimensional nature of spine deformity by measuring the curve gravity in both the frontal and the sagittal plane [17]. However, repeating a 2D analysis twice is not a substitute for a true three-dimensional analysis. Finally, three-dimensional analysis of the brace effect was also conducted [18] by using a set of clinical indices extracted from three-dimensional reconstructions of the spine. However, those clinical indices were not independent, which made effect localization and analysis difficult. Moreover, brace effect variability itself was not studied.

To overcome all these limitations, we propose to study the statistical variability of the spine shape and of the spine shape deformation using local features that describe both the position and the orientation of the vertebrae (i.e. rigid transformations). However, mathematical and computational tools need to be developed because conventional statistical methods usually apply under the assumption that the embedding space is a vector space where addition and scalar multiplication are defined. Unfortunately, this is not the case for rigid transformations. For example, the conventional mean is not applicable to rigid transformations since it would involve the addition of the measures followed by a division by the sample size.

Recently, many researchers have been working towards the generalization of mathematical tools on Lie groups and Riemannian manifolds. A general framework for the development of probabilistic and statistical tools on Riemannian manifolds was recently proposed [19], [20]. Riemannian manifolds are more general than Lie Groups, thus findings realised on Riemannian manifolds also apply to Lie groups (and to rigid transformations by extension). Concepts such as the mean, covariance and normal distribution have been formalized for Riemannian manifolds. Many studies were realized more specifically for the tensors space, because of the develop-

ment of Diffusion Tensor Imaging (for example: [21]–[25] and references therein). The idea of computing statistics on manifolds was also used to perform anatomical shape analysis. For example, this idea can be found in our previous work [26] where an analysis of the spine shape anatomy based on Lie groups properties was proposed and in the work of Fletcher et al. [27] where a generalization of the PCA was introduced and applied to the analysis of medial axis representations of the hippocampus. However, a Riemannian approach to the study of articulated models of the spine shape was never used.

To our knowledge, no previous work reported a variability analysis of the scoliotic spine shape and of the scoliotic spine shape deformations using rigid transformations as geometric descriptors. In that context, the contributions of this paper are: to introduce a new model of the variability of spine shapes and of spine shape deformations based on well posed statistics on a suitable articulated shape model, to suggest a method to compare the variability between different groups of patients, to propose a 3D visualization method of this variability and, last but not least, to present the resulting variability models computed using large groups of scoliotic patients.

II. MATERIAL AND METHODS

This section presents the material and methods used to construct and analyze variability models of the spine shape. We will first describe the method used to create articulated models representing the spine from pairs of radiographs. The procedure used to create variability models from samples of articulated spine shapes will then be presented. Since our articulated shape models do not naturally belong to a vector space, conventional statistical methods could not be applied. However, it is still possible to define distances between articulated shape models. Therefore, some statistical notions had to be generalized based on the concept of distance between primitives. Riemannian geometry offers a good framework for this purpose. Thus, centrality and dispersion measures applied to Riemannian manifolds and their specialization to articulated models will be introduced. Finally, the visualization and the quantitative comparison of variability models built from articulated spine shapes will be discussed.

A. Articulated Shape Models of the Spine from Multiple Radiographs

Multi-planar radiography is a simple technique where two (or more) calibrated radiographs of a patient are taken to compute the 3D position of anatomical landmarks using a stereo-triangulation algorithm. It is one of the few imaging modalities that can be used to infer the three-dimensional anatomy of the spine when the patient is standing up. Furthermore, bi-planar radiography of scoliotic patients is routinely performed at Sainte-Justine hospital (Montreal, Canada). Thus, a large amount of data is available for analysis.

In the case of bi-planar radiography of the spine, six anatomical landmarks are identified on each vertebra from T1 (first thoracic vertebra) to L5 (last lumbar vertebra) on a posterior-anterior and a lateral radiograph. The 3D coordinates of the landmarks are then computed and the deformation of

a high-resolution template using dual kriging yields 16 additional reconstructed landmarks. The accuracy of this method was previously established to 2.6 mm [28].

Once the landmarks are reconstructed in 3D, we rigidly registered registered each vertebrae to its first upper neighbour and the resulting rigid transforms were recorded. By doing so, the spine is represented by a *vector of inter-vertebral rigid transformations* $S = [T_1, T_2, \dots, T_N]$ (see Fig. 2). This representation is especially well adapted to an analysis of the anatomical variability since the inter-vertebral rigid transformations describe the state of the physical links that are modified by the pathology and alter the shape of the whole spine.

Most scoliotic patients are adolescents or pre-adolescents. Thus, spine length of patients afflicted by scoliosis varies considerably. In order to factor out that variability source from the statistical analysis, one could be tempted to normalize the articulated models. On the one hand, this could be desirable since the global spine size is associated primarily with patients' growth and most physicians are more interested in analyzing the variability linked to the pathology. On the other hand, the development of many musculoskeletal pathologies, for instance adolescent idiopathic scoliosis, is tightly linked with the patient growth process. Thus, normalization could discard valuable information. Furthermore, preliminary experiments revealed that, with scoliotic patients, the only notable effect of normalization was found along the axial direction where the translational variability was almost eliminated (a reduction ranging from 3.0 mm^2 in the thoracic region to 8 mm^2 in the lumbar region). In summary, normalization could be desirable in certain situations, but it did not led to more probative results in our application. Thus, to preserve the clear physical interpretation of the variability models we chose not to normalize the articulated spine models.

The vector S enables a local analysis of the links between the vertebrae. However, it is sometimes preferable to analyze the spine shape using absolute instead of relative transformations. For example, posture analysis is simpler when one uses absolute transformations. However, it is easy to convert S into an absolute representation $S_{absolute}$ using recursive compositions (where \circ is the operator of composition).

$$S_{absolute} = [T_1, T_1 \circ T_2, \dots, T_1 \circ T_2 \circ \dots \circ T_N] \quad (1)$$

The transformations are then expressed in the local coordinate system of the lowest vertebra. The choice of this reference coordinate system is arbitrary, but it can be changed easily based on the application needs.

To study spine shape deformations caused by the progression of the pathology or by a treatment, we need to compute the "differences" between shape models. This can be realised once again using a *vector of rigid transformations*. Let $S = [T_1, T_2, \dots, T_N]$ and $S' = [T'_1, T'_2, \dots, T'_N]$ be two vectors of rigid transformations extracted from two different radiological exams of the same patient (before and after a surgery, for instance), then another vector of rigid transformations can be defined with the transformations that turn the elements of S into the corresponding elements of S' (see Fig. 2).

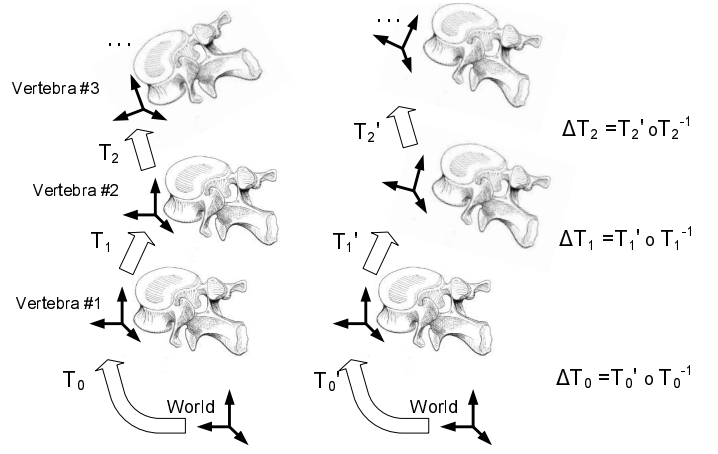


Fig. 2. Spine shape and spine shape deformation expressed using rigid transformations

The resulting vector ΔS will only depend on the difference between the two 3D spine geometries and not on the anatomy of the patient.

$$\Delta S = [\Delta T_1, \Delta T_2, \dots, \Delta T_N] \quad \text{with} \quad \Delta T_i = T'_i \circ T_i^{-1} \quad (2)$$

Since this vector is still a vector of rigid transformations the analysis performed on S could also be performed on ΔS to study spine shape modifications.

B. Statistics on Rigid Transforms and Articulated Models

The articulated shape models that are constructed from stereo-radiographs are vectors of rigid transformations and there is no addition or scalar multiplication defined between them. Therefore, conventional statistics do not apply. However, rigid transformations belong to a Riemannian manifold and Riemannian geometry concepts can be efficiently applied to generalize statistical notions to articulated shape models of the spine.

To use a Riemannian framework, we need to define a suitable distance and to find the structure of the geodesics on the manifold. To achieve this task, we introduce two representations of rigid transformations.

First, a rigid transform is the combination of a rotation R and a translation t . The action of a rigid transform on a point is usually written as $y = Rx + t$ where $R \in \mathcal{SO}^3$ and $x, y, t \in \mathbb{R}^3$. Thus, a simple representation of a rigid transform would be $T = \{R, t\}$. Using this representation composition and inversion operations have simple forms (respectively, $T_1 \circ T_2 = \{R_1 R_2, R_1 t_2 + t_1\}$ and $T^{-1} = \{R^T, -R^T t\}$).

Another way to represent a rigid transformation is to use a rotation vector instead of the rotation matrix. The rotation vector representation is based on the fact that a 3D rotation can be fully described by an axis of rotation supported by a unit vector n and an angle of rotation θ . The rotation vector r is defined as the product of n and θ . So we have a representation $\vec{T} = \{r, t\} = \{\theta n, t\}$.

The conversion between the two representations is simple since the rotation vector can be converted into a rotation matrix

using Rodrigues' formula (numerical implementation details can be found in [29]):

$$R = I + \sin(\theta) \cdot S(n) + (1 - \cos(\theta)) \cdot S^2(n) \quad (3)$$

$$\text{where } S(n) = \begin{bmatrix} 0 & -n_z & n_y \\ n_z & 0 & -n_x \\ -n_y & n_x & 0 \end{bmatrix}$$

And the inverse map (from a rotation matrix to a rotation vector) is given by the following equations:

$$\theta = \arccos\left(\frac{\text{Tr}(R) - 1}{2}\right) \quad \text{and} \quad S(n) = \frac{R - R^T}{2 \sin(\theta)} \quad (4)$$

A left-invariant distance ($d(T_1, T_2) = d(T_3 \circ T_1, T_3 \circ T_2)$) between two rigid transforms can easily be defined from the rotation vector representation:

$$d(\vec{T}_1, \vec{T}_2) = N_\lambda(\vec{T}_2^{-1} \circ \vec{T}_1) \quad (5)$$

$$\text{with: } N_\lambda(\vec{T})^2 = N_\lambda(\{r, t\})^2 = \|r\|^2 + \|\lambda t\|^2$$

The parameter λ is a real number that controls the relative weight of the translation and rotation in the computation of the distance. Because the rotation vector and the translation do not have the same units it can also be understood as a unit conversion constant. Preliminary experiments showed that our results are not sensitive the exact value of λ (values ranging from 0.01 to 1 were assessed). Thus, unless otherwise noted, λ was set to 0.05 since this value leads to approximatively equal contributions of the rotation and the translation to the variance.

To use the Riemannian machinery described in [20], the exponential map Exp_x and the logarithmic map Log_x associated with the distance presented at Equation 5 are also needed. Those two maps connect the manifold itself and its tangent spaces. They can be understood as the folding (Exp_x) and unfolding (Log_x) operations that connect the tangent space at x to the manifold. More formal definitions of those two maps based on a Riemannian metric can be found in the Appendix.

In the general case, one would have to solve a system of partial differential equations (see Equation 14 in the Appendix). However, in our case, there is no interaction between the translational and rotational part of the rigid transformation involved in the computation of the norm (more formally, the local representation of the metric is a block diagonal matrix formed by the local representation of the metric on rotations and the local representation of the metric on translations). Therefore, the geodesics for this distance are the Cartesian product of the geodesics of the rotation and translation parts of the rigid transforms.

The geodesics of the translational part are simply straight lines since translation belongs to a vector space. The rotational part is slightly more complex. However, because the selected distance between the rotations is left and right invariant, their Exp and Log maps correspond to the conversion between a rotation matrix and the corresponding rotation vector and, thanks to the Rodrigues' Formula 3, these computations can be done very efficiently.

Moreover, $\text{Exp}_x(\vec{T}) = \text{Exp}_{Id}(\vec{x}^{-1} \circ \vec{T})$ and $\text{Log}_x(T) = \text{Log}_{Id}(x^{-1} \circ T)$ since the distance of Equation 5 is left-invariant. Finally, Exp_{Id} and Log_{Id} are the conversions between the rotation vector and the rotation matrix combined with a scaled version of the translation vector.

$$\text{Exp}_{Id}(\vec{T}) = \begin{bmatrix} R(r) \\ t \end{bmatrix} \quad \text{and} \quad \text{Log}_{Id}(T) = \begin{bmatrix} r(R) \\ \lambda t \end{bmatrix} \quad (6)$$

1) *Centrality*: The next step to build a variability model is to define a centrality measure. Because scalar multiplication and addition are not defined on rigid transformations, the conventional mean cannot be used. A generalization of the mean that can be applied to Riemannian manifolds is thus needed.

It can be observed that the conventional mean (defined on vector spaces) minimizes the Euclidian distance of the measures with the mean. Thus, when given a distance, a generalization of the usual mean can be obtained by defining the mean as the element μ of a manifold \mathcal{M} that minimizes the sum of the distances with a set of elements $x_{0\dots N}$ of the same manifold \mathcal{M} .

$$\mu = \arg \min_{x \in \mathcal{M}} \sum_{i=0}^N d(x, x_i)^2 \quad (7)$$

This generalization of the mean, called the Fréchet mean [30], is equivalent to the conventional mean for vector spaces with a Euclidian distance. However, when it is applied to more general Riemannian manifolds, the mean is no longer guaranteed to be unique. Indeed, the mean is the result of a minimisation; therefore more than one minimum can exist. However, Kendall [31] showed that the Fréchet mean exist and is unique if the data is sufficiently localized.

The computation of the Fréchet mean directly from the definition is difficult because of the presence of a minimization operator. Hopefully, a simple gradient descent procedure can be used to compute the mean [19]. This procedure is summarized by the following recurrent equation:

$$\mu_{n+1} = \text{Exp}_{\mu_n} \left(\frac{1}{N} \sum_{i=0}^N \text{Log}_{\mu_n}(x_i) \right) \quad (8)$$

The equation is guaranteed to converge. Moreover, in practice it converges rather quickly (for instance convergence is generally obtained in less than five iterations for rigid transformations).

To use Equation 8 one has to initialize the mean to start the procedure. The initial value can be one of the point of the set in which the mean is to be computed. Furthermore, more than one starting point can be tried to test the uniqueness of the mean and escape local minimums.

2) *Dispersion*: In addition to the centrality measure given by the Fréchet mean, a dispersion measure is also needed to perform most tasks of practical interest. Since the mean is computed based on the minimisation of the distance between a set of primitives and the mean, then the variance can be defined as the expectation of that distance.

$$\sigma^2 = E [d(\mu, x)^2] = \frac{1}{N} \sum_{i=0}^N d(\mu, x_i)^2 \quad (9)$$

A directional dispersion measure would also be needed in most cases, because the anatomical variability is expected to be greater in some directions. The covariance is usually defined as the expectation of the matricial product of the vectors from the mean to the elements on which the covariance is computed. Thus, a similar definition for Riemannian manifolds would be to compute the expectation in the tangent space of the mean using the Log map:

$$\begin{aligned} \Sigma &= E [\text{Log}_\mu(x)^T \text{Log}_\mu(x)] \\ &= \frac{1}{N} \sum_{i=0}^N \text{Log}_\mu(x_i)^T \text{Log}_\mu(x_i) \end{aligned} \quad (10)$$

This generalized covariance computed in the tangent space of the mean and the associated variance are connected since $\text{Tr}(\Sigma) = \sigma^2$, which is also the case for the usual vector space definitions.

3) *Extrinsic Approximations*: The Riemannian approach enables a statistical analysis that is intrinsic to the manifold. Furthermore, it provides a rationale to the choice of algorithms and representations used to work on rigid transformations. However, it also leads to an iterative scheme to compute the mean, while *ad hoc* but computationally more efficient methods to average 3D rotations also exist.

These methods are based on the computation of the mean of an extrinsic representation of 3D rotations. The two most frequently used are the computation of the mean rotation matrix (followed by an SVD renormalization) and of the mean unit quaternion. Theoretically, those methods do not lead to the same result and are not stable with respect to a reference frame shift. Nevertheless, simulation experiments were performed for those two extrinsic methods by Eggert et al. [32] in a registration context and by Gramkow [33] to compare the intrinsic mean and those two extrinsic methods. These simulations showed that the results were similar when the standard deviation of rotations was less than 40 degrees. Therefore, if speed is a concern and only small differences of orientation are expected for a given application, then one would be justified to approximate the Fréchet mean by a more computationally efficient approximation.

C. Visualization of the Statistical Models of the Spine

The mean spine shape model is easily visualized by reconstructing a 3D spine model with standard surface models of vertebrae separated by the associated mean inter-vertebral transforms. However, the mean spine shape deformations are small and a direct visualisation of those would be difficult. Therefore, the mean spine shape deformations are visualized by reconstructing a mean model before and after deformation.

The generalized covariance matrix associated with a single rigid transform is a six by six matrix. Thus, an intuitive visualization of the whole covariance matrix is difficult. However, the upper left and lower right quarters of this matrix are three

by three tensors and can easily be visualized in 3D using an ellipsoid. The principal axes of these ellipsoids are the eigenvectors scaled by the corresponding eigenvalues. The extent of the first ellipsoid (associated with the rotation) in a given direction is the angular variability around that axis and the extent of the second ellipsoid (associated with the translation) in a given direction is the translational variability along that direction.

Because, the first tensor is the covariance of the rotation and the second tensor is the covariance of the translation this visualisation is quite intuitive and can be understood by people without strong mathematical backgrounds. The drawback of this visualisation is that the coupling between the rotation and the translation is lost during the visualisation process. However, preliminary tests indicated that, for the specific case of the spine anatomy and treatment modelling, the amount of variance explained by this coupling is small compared to those of the rotation and of the translation.

D. Comparing Statistical Models of the Effect of Orthopaedic Treatments

In addition to the qualitative visualisation of the variability models, it would be very interesting to compare two sets of rigid transformations used to model the spine shape deformations in order to locate significant “differences”.

It could be observed that, unlike inter-vertebral transformations, the rigid transformations associated with the effect of orthopaedic treatments are usually small so the manifold locally looks like a vector space. This observation enables us to approximate hypothesis tests on rigid transforms modelling spine shape deformations with hypothesis tests developed for vector spaces. More formally, it was shown that a normal distribution on a Riemannian manifold could be approximated by a vector space normal distribution if the Ricci curvature matrix is small compared to the inverse of the covariance [20].

The T^2 test and the Box’s M test are commonly used to compare the mean and the covariance of multivariate datasets [34]. Those two tests operate under the assumption that both datasets have normal distributions. Therefore, if one finds a tangent space where both datasets can be approximated by a normal distribution, then it is justified to use those tests. For that purpose, we performed the T^2 and M tests in the tangent space of the Fréchet of the union of both datasets. There is no guarantee that it is the best tangent space to obtain normal distributions and other choices may be justifiable in other applications. However, this tangent space is a good compromise since it minimises the non-linearities associated with large rotations in both sets. The normality assumption was tested using Lilliefors tests [35] with a significance level of 5%. Moreover, hypothesis tests based on the T^2 statistic often assume that the covariance matrices of the two samples are equal, which is not always true in our experiments. The T^2 test described by Nel and Van der Merwe [36] was thus selected since it is not based on that assumption.

The use of non-parametric tests on distances between the primitives, like this was done by Terriberry et al. [37] on medial axis representations of the lateral ventricles, could

have been a possible alternative to the T^2 test. However, the statistical power of non-parametric tests based solely on distances is generally inferior, therefore parametric tests were preferred.

The variance of the treatment effect is also relevant to analyze because it is expected to be greater than the one of the motion observed between two reconstructions without treatment (if the treatment is efficient). A one-sided test on the variances was thus performed by applying a rank sum test [35] to the squared norm of the rigid transformations expressed in the tangent space of the mean.

In addition to testing for differences between the mean, covariance and variance, it would also be interesting to test if post-treatment groups are on average closer to the mean of a group of healthier patients than pre-treatment groups. It would be unethical to expose healthy subjects without therapeutic reasons to ionizing radiation in order to build a healthy spine model. Thus, it was decided to compare pre-treatment and post-treatment groups with the mean spine shape of a healthier group of patients. This healthier group was composed of patients that were diagnosed with very mild scoliosis (Cobb angle [10] of less than 30 degrees) and did not receive any treatment. These patients had a radiographic examination prescribed for diagnostic purposes; therefore no additional radiation exposure was needed. The distance between the mean spine model of this group and another articulated model could be regarded as a *distance to normality*. The distance used is the one described in equation 5 with $\lambda = 0.005$ (to limit the bias introduced by having patient samples with different age distributions). This distance to normality was then computed on pre-treatment and post-treatment reconstructions of patients that received either a Boston brace or a Cotrel-Dubousset instrumentation. The differences between pre and post treatment groups was then tested for statistical significance using a sign test [35] which can cope with the unknown but asymmetrical distribution of the differences.

A relatively large number of hypothesis tests were performed in this study, thus false positives could become a problem and needs to be controlled. The most common method to control false positives is to control the family wise error rate (FWER), which is the probability of having one or more false positives among all the tested hypotheses (see Shaffer [38] for a review of many methods to control the FWER). However, the FWER offers an extremely strict criterion, which is not always appropriate and results in a drastic reduction of the statistical power of individual tests. Benjamini and Hochberg [39] proposed an alternative to the control of the FWER where one controls the accumulation of false positives relative to the number of significant tests. However, the original method of Benjamini and Hochberg did not take into account that an unknown proportion of the tests can be expected to be significant, which is our case since orthopedic treatments are expected to have an effect on the spine shape. Furthermore, their method assumes that all tests are independent, which might not be true in this case if the orthopedic treatments altered the patients' standing posture. Fernando et al. [40] recently proposed a method to control the proportion of false positives (PFP) which does not depend on

the correlation structure between the tests and that takes into account the proportion of true null hypothesis out of all the tested hypothesis. The numerical values of the PFP will let us determine if the significance levels chosen are stringent enough with respect to our tolerance to false positives. The PFP for a significance level α can be computed using the following equation:

$$P\hat{F}P_\alpha = \frac{\alpha k \hat{p}_0}{R_\alpha} \quad (11)$$

where k denotes the number of tests performed, R_α the number of null hypothesis rejected for a level of significance α and \hat{p}_0 the estimated proportion of true null hypothesis. The value of k , α and R_α are readily available and \hat{p}_0 was estimated based on the distribution of the p-values using the method described in Mosig et al. [41].

III. RESULTS

The methodology described in the previous sections was applied to four groups of scoliotic patients of the Montreal's Sainte-Justine Hospital. The selection of the patients included in these groups was based on the availability of the radiographs needed to compute 3D reconstructions of the spine. The main characteristics of these groups are the following:

- I) A group of 295 scoliotic patients who had biplanar radiographs at least once.
- II) A group of 39 patients who had biplanar radiographs while wearing a Boston brace and without it on the same day.
- III) A group of 33 patients that had a Cotrel-Dubousset corrective instrumentation surgically installed and had biplanar radiographs taken before and after the surgery (with less than 6 months between the two examinations).
- IV) A group of 26 untreated scoliotic patients who had biplanar radiographs two times within 6 months.

A. Geometric Variability of the Scoliotic Spine Anatomy

A variability model of the scoliotic spine shape anatomy was computed using the group I. The mean spine shape and the variability based on relative transformations are illustrated in Fig. 3, where it can be observed that the mean shape has curvatures in the lateral and frontal plane. The curvatures in the lateral plane correspond to healthy kyphosis and lordosis, but the light curve in the frontal plane is not part of the normal anatomy of the spine and is caused by scoliosis. It is also interesting to note that the curve is on the right side because there is more right thoracic curves than left thoracic curves among scoliotic patients. The variability is also inhomogeneous (it varies from a vertebra to another) and anisotropic (stronger variability in some directions). The strongest translational variability is found along the axial direction and one can also observe from Fig. 3 that the main extension of the rotation vector covariance ellipsoid is along the anterior-posterior axis, which indicates that the main rotation variability is around this axis (as it could be expected for scoliosis).

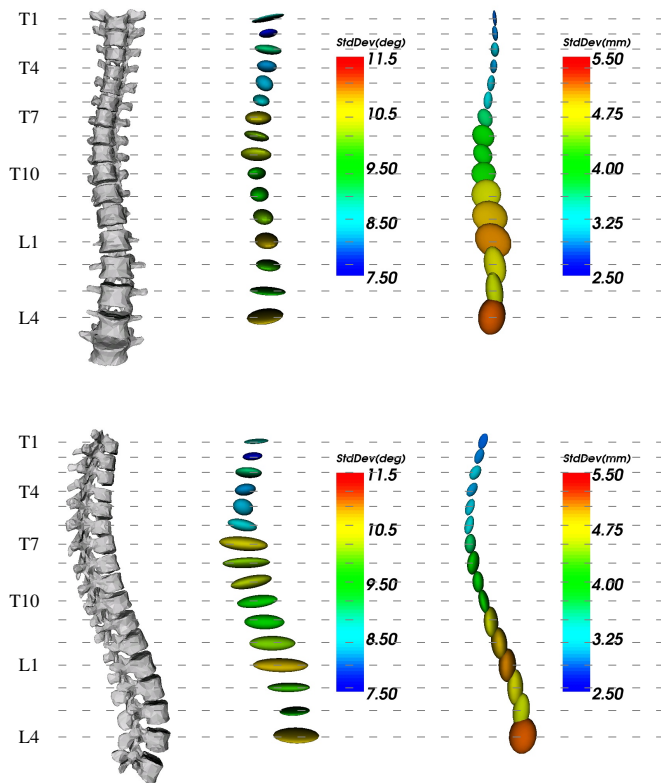


Fig. 3. Statistical model of the inter-vertebral poses for group I. From left to right: mean spine model, rotation and translation covariance. Top: frontal view. Bottom: sagittal view.

Complementary information can also be extracted from a model based on absolute positions and orientations of the vertebrae, as illustrated in Fig. 4 (with the reference coordinate system fixed to the lowest vertebrae). As it was expected, the mean of this second model is very similar to the mean of the model based on the relative positions and orientations. However, the variabilities are greater, which is normal since the vertebrae on top are farther away from the reference frame. Furthermore, the relative contributions to the global variability of the translational variability in the coronal direction and of the rotational variability in the sagittal direction are more important. One could also notice that the rotational variability is maximal in the middle of the spine (around T10) and not on the top, which might be the result of patients' tendency to keep their head and shoulders straight during the radiological examination.

B. Geometric Variability of the Spine Shape Deformations

In addition to the analysis of the spine anatomy, the method described in this document can also be used to analyze deformations of the spine (for example, the deformations associated with the outcome of orthopaedic treatments). To do so, one could compare the spine shape models computed for all subjects before and after the deformation (before and after treatment). However, inter-patient variability would hide the variability that is intrinsic to the deformation process. To reduce the effect of the inter-patient variability, the de-

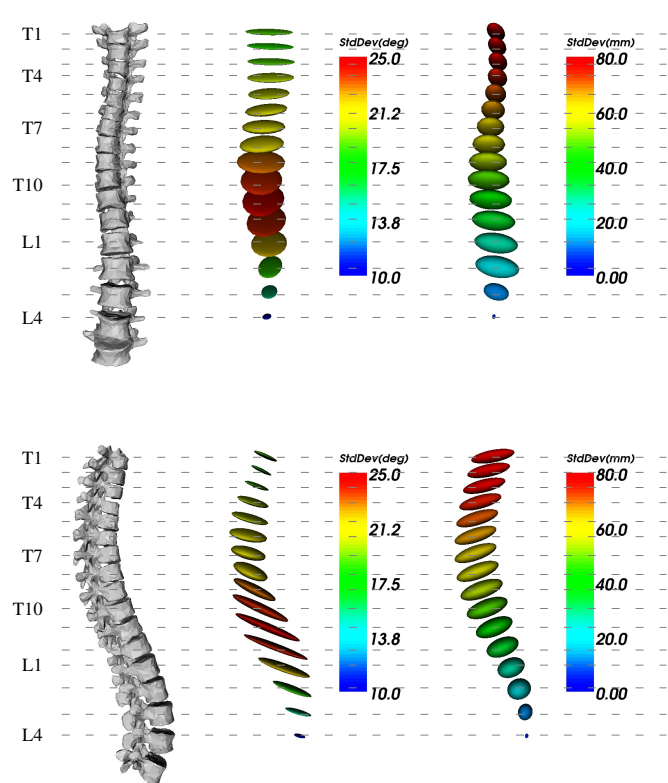


Fig. 4. Statistical model of the absolute vertebral poses for group I (with reference frame at L5). From left to right: mean spine model, rotation and translation covariance. Top: frontal view. Bottom: sagittal view.

formation is defined as a vector of rigid transformations that transforms the spine shape before into the spine shape after deformation for a given patient (see Fig. 2 and Equation 2). Then, a statistical analysis of these rigid transformations is performed on each patients group. Two treatments (the Boston brace and the Cotrel–Dubousset instrumentation) and a control group (untreated patients) were analyzed that way.

1) *Boston Brace*: The Boston brace is a treatment that is prescribed for patients with mild to moderate scoliosis. In order to validate the brace design and adjustment, biplanar radiographs of the patients are taken with and without brace. We thus used those radiographs to construct a statistical model of the spine shape deformations associated with the brace without exposing the patients to additional doses of radiation. This model is illustrated by Fig. 5. It could be observed from this model that the variability of the Boston brace effect is more important in the lower part of the thoracic spine (approximately from T7 to L1, with a maximum at T11). Moreover, the mean curve in frontal view seems to be reduced by the treatment. However, the healthy kyphosis and lordosis found in the sagittal view are also reduced which is not a desirable effect (from a medical perspective).

2) *Cotrel-Dubousset Surgery*: The surgical treatment that was used is the installation of a Cotrel–Dubousset instrumentation. Other types of instrumentations also exist, however the Cotrel–Dubousset type is the most common in North America and is the type of surgery for which the highest number of

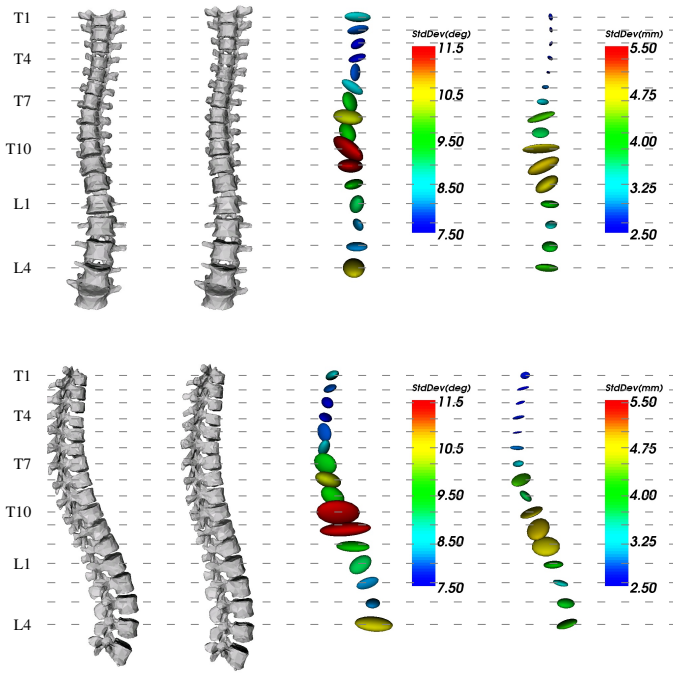


Fig. 5. Statistical model of the spine shape deformations associated with the Boston brace. From left to right: mean shape prior treatment, mean shape with the brace, rotation and translation covariance of the spine shape deformations. Top: Frontal view. Bottom: sagittal view

cases were available. The variability model of the effect of the Cotrel-Dubousset surgery is illustrated at Fig. 6. It comes with no surprise that the variability of the treatment effect is greater for the Cotrel-Dubousset surgery than it is for the brace, since the surgery is a more invasive treatment that is reserved for severe cases. Furthermore, it is interesting to note that the variability reaches its maximum at T12, two vertebrae lower than for the Boston brace. Unlike the Boston brace, the Cotrel-Dubousset treatment preserved the mean curves in the sagittal view.

3) *Untreated Patients:* The spine shape deformation model computed for the Boston brace and the Cotrel-Dubousset surgery were influenced by variability sources other than the treatment itself such as patient posture, growth stage and 3D reconstruction error. To assess the relative importance of those sources of variability a group of 26 untreated patients, whom had two biplanar radiographs examinations with at most six months between them, were used to analyze the deformation progression without treatment. The results are illustrated in Fig. 7. The variability for $L5 \rightarrow L4$ was removed from Fig. 7 because it was corrupted by an artifact of the 3D reconstruction process. As it was expected, the mean spine shapes for the two examinations are very similar and the variability of the spine shape deformation appears to be much smaller than the ones associated with the Boston brace or the Cotrel-Dubousset surgery.

4) *Comparison of the Effect of Treatments between Groups:* The presence of a group of untreated patients enables us to test for significant effect of a treatment on our centrality and dispersion measure (respectively the Fréchet mean and the

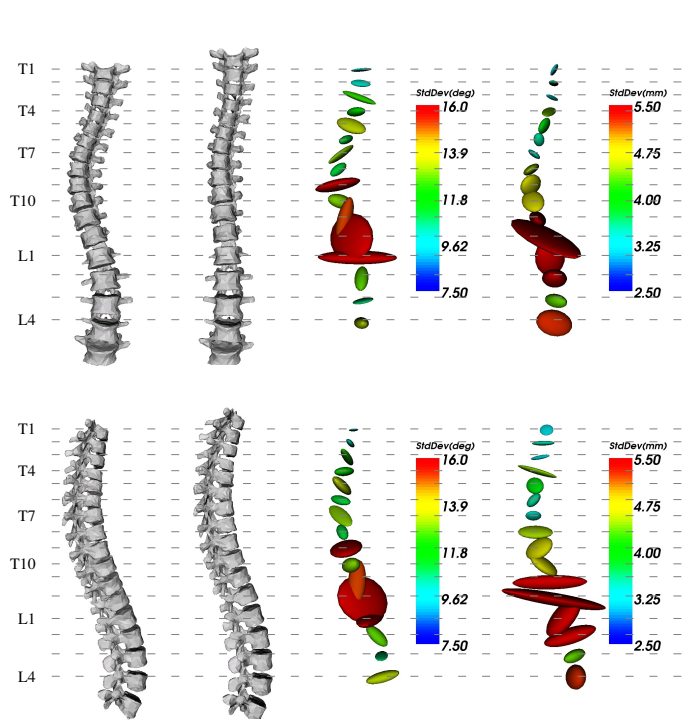


Fig. 6. Statistical model of the spine shape deformations associated with the Cotrel-Dubousset instrumentation. From left to right: mean shape before surgery, mean shape after surgery, rotation and translation covariance of the spine shape deformations. Top: Frontal view. Bottom: sagittal view

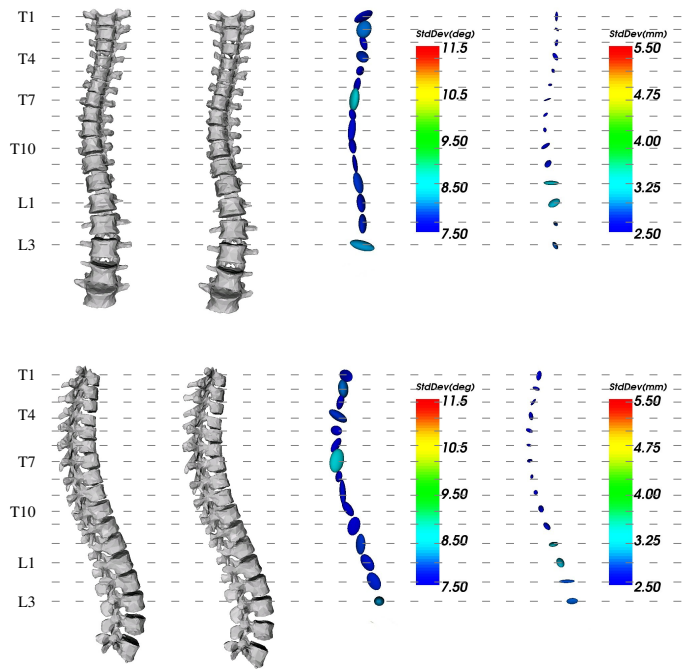


Fig. 7. Statistical model of scoliosis progression without treatment. From left to right: mean shape at the first examination, mean shape at the second examination, rotation and translation covariance of the spine shape deformations. Top: Frontal view. Bottom: sagittal view

generalized covariance).

Since the variances are small and the means are near zero, the non-linearities linked to the manifold curvature are small, so the Hotelling's T^2 test and Box's M test were used to test for significant differences between the untreated group and the two other groups (the null hypothesis being that they are not different). The results are reported in table I where p-values lower than 0.01 are marked with a star ("*"), p-values lower than 0.001 are marked with a two stars and p-values lower than 0.0001 are marked with a three stars.

The table I shows that the Boston brace has a significant effect on the mean shape and on the variability for two different regions of the spine, respectively from T1 to T6 and from T8 to T12. The Cotrel-Dubousset surgery appeared to have a very sparse effect on the mean shape, however it has a significant effect on the variability of the spine shape deformation for all studied vertebral levels.

Table II presents the difference between the distance to normality before receiving a treatment and after receiving the treatment. The table II also introduces the significance of this distance reduction (p-value computed from a one-sided sign test). The total row is computed by considering the summation of the distances for all inter-vertebral levels. The reduction of the distance to normality range from 3% to 34% for the Cotrel-Dubousset instrumentation and from -12 % to 11 % for the Boston brace. This table seems to indicate that a Cotrel-Dubousset instrumentation deforms the spine of the patients toward the mean shape of the healthier group. However, this reduction is not significant for many inter-vertebral levels. In the case of the Boston brace no significant reduction was found.

The PFP numerical values (Eq. 11) for significance level of 0.01, 0.001 and 0.0001 (the three significance levels used in this study) computed from all tests results presented are respectively of 0.00167, 0.000257 and 0.0000423. This means that a significance level of 0.01 on individual tests will lead on average (if we were to repeat this study many times) to 1 false positive for every 600 rejected null hypothesis.

C. Quantification of the Reconstruction Error

The anatomical landmarks reconstruction error induces variability on inter-vertebral transforms. However, we are interested in the variability that is intrinsic to the patients. Thus, we ran computer simulations to assess the relative effect of reconstruction error on the computed variability.

The 3D reconstruction method used to compute the 3D coordinates of the anatomical landmarks was previously validated and the mean error on the landmarks reconstruction was evaluated to 2.6 mm [28]. So, we simulated virtual spine models with mean reconstruction errors from 0.25 mm to 5 mm and we computed the variabilities of the corresponding spine shapes and spine shape deformations models.

The augmentation of the simulated error had a linear effect on the standard deviations of the corresponding rigid transformations. In the case of spine shape model, the standard deviation of the translational part varied from the 0.1 to 2 mm and the rotational part varied from 0.2 to 3.9 degrees. The

TABLE II

REDUCTION OF THE DISTANCE TO AN HEALTHIER SPINE SHAPE BETWEEN PRE AND POST TREATMENT GROUPS AND THE ASSOCIATED SIGNIFICANCE OF THIS REDUCTION (EXPRESSED AS A P-VALUE). ONE STAR INDICATES A P-VALUE LOWER THAN 0.01, TWO STARS INDICATES A P-VALUE LOWER THAN 0.001 AND THREE STARS INDICATES A P-VALUE LOWER THAN 0.0001

Inter-vertebral levels	Cotrel-Dubousset		Boston Brace	
	Reduction	p-value	Reduction	p-value
T2 →T1	3.0 %	6.3e-1	3.0 %	5.0e-1
T3 →T2	8.5 %	1.4e-1	-9.6 %	5.0e-1
T4 →T3	27.9 %	4.1e-2	5.2 %	1.0e-1
T5 →T4	24.5 %	2.5e-4 **	10.6 %	5.5e-2
T6 →T5	13.3 %	8.2e-2	9.3 %	2.7e-2
T7 →T6	24.8 %	8.2e-2	-7.9 %	5.0e-1
T8 →T7	17.4 %	1.5e-1	11.4 %	3.7e-1
T9 →T8	18.2 %	4.1e-2	-6.3 %	5.0e-1
T10→T9	34.4 %	2.5e-4 **	10.8 %	2.6e-1
T11→T10	9.3 %	4.1e-2	7.6 %	5.0e-1
T12→T11	31.2 %	7.4e-3 *	5.6 %	1.7e-1
L1 →T12	33.7 %	7.4e-3 *	0.5 %	5.0e-1
L2 →L1	24.6 %	8.2e-2	8.4 %	1.0e-1
L3 →L2	20.7 %	8.2e-2	-12.2 %	8.3e-1
L4 →L3	27.7 %	4.1e-2	7.1 %	5.0e-1
Total	23.3 %	2.5e-4 **	3.3 %	1.0e-1

spine shape deformation model was a little bit more sensitive to the reconstruction error since the standard deviations of the translational part varied from 0.1 to 2.5 mm and the rotational part varied from 0.2 to 5.3 degrees.

In summary, with error levels compatible with the previous validation studies, all simulated variances are way below the variabilities observed from scoliotic patients. Therefore, the observed variabilities are mainly associated sources intrinsic to the patients and not with 3D reconstruction errors.

IV. DISCUSSION

A. Variability Sources

The models used in this study describe the variability of the observed 3D spine shape. This variability is partially the result of the anatomical variability inherent to the pathology, but other causes were also present.

Scoliosis is very often diagnosed during puberty, thus growth status is likely to be a significant variability factor. This was confirmed by the fact that the maximal translational variability is along the axial direction.

The posture during the acquisition was standardized, but a certain proportion of the variability might be the result of small differences between patients' postures during the stereo-radiographic exams. Scoliotic patients are however known to have postural problems, so the variability caused by differences in the posture and the variability caused by scoliosis might be hard to discern.

The anatomical landmarks 3D reconstruction error is also a source of variability. However, the variances simulated from synthetic data with a controlled 3D reconstruction error are well below the variabilities computed from real patients. The observed variabilities are thus mainly associated with spine geometry and not with 3D reconstruction errors.

TABLE I

STATISTICAL SIGNIFICANCE (EXPRESSED USING P-VALUES) OF THE DIFFERENCE BETWEEN THE MEANS AND THE COVARIANCE MATRICES OF A CONTROL GROUP (IV), A GROUP OF PATIENTS WEARING A BOSTON BRACE (II) AND A GROUP THAT HAD A COTREL-DUBOUSSET INSTRUMENTATION SURGICALLY INSTALLED (III). P-VALUES FOR INTER-VERTEBRAL LEVELS MARKED WITH A γ SHOULD BE INTERPRETED WITH CAUTION SINCE THE NORMALITY TEST FAILED. ONE STAR INDICATES A P-VALUE LOWER THAN 0.01, TWO STARS INDICATES A P-VALUE LOWER THAN 0.001 AND THREE STARS INDICATES A P-VALUE LOWER THAN 0.0001

Inter-vertebral levels	IV vs II			IV vs III		
	Mean	Covariance	Variance	Mean	Covariance	Variance
T2 →T1	2.3e-4 **	1.1e-1	3.7e-2	4.7e-3 *	3.8e-4 **	4.5e-2
T3 →T2	2.4e-3 *	5.6e-2	1.1e-1	1.9e-3 *	6.3e-3 *	1.1e-3 *
T4 →T3	9.5e-9 ***	1.4e-2	4.0e-1	6.0e-4 γ **	3.8e-8 γ ***	1.5e-3 *
T5 →T4	2.2e-3 γ *	1.8e-1 γ	7.4e-1	1.3e-1	1.1e-3 *	6.6e-3 *
T6 →T5	6.1e-3 *	1.7e-1	1.1e-1	7.2e-1	5.4e-6 ***	1.5e-6 ***
T7 →T6	1.3e-2	1.3e-1	1.4e-2	4.9e-1	7.3e-4 **	1.2e-4 **
T8 →T7	6.0e-2	4.3e-2	2.4e-2	1.1e-2	8.1e-4 **	5.9e-3 *
T9 →T8	4.9e-1	7.5e-6 ***	1.1e-5 ***	1.6e-1	1.5e-7 ***	3.7e-6 ***
T10→T9	2.4e-1	5.2e-4 **	5.1e-4 **	2.0e-2	1.5e-10 ***	6.8e-6 ***
T11→T10	3.7e-1 γ	2.3e-5 γ ***	1.3e-4 **	1.3e-1	2.2e-7 ***	8.6e-7 ***
T12→T11	8.2e-1 γ	4.4e-6 γ ***	3.3e-5 ***	8.4e-2	1.0e-9 ***	1.4e-6 ***
L1 →T12	6.8e-1	5.3e-4 **	1.5e-3 *	3.1e-1	5.8e-11 ***	2.5e-5 ***
L2 →L1	9.3e-1	2.9e-1	2.4e-2	1.9e-1	2.1e-8 ***	3.8e-5 ***
L3 →L2	2.7e-2	2.9e-1	1.4e-1	4.5e-5 ***	2.3e-6 ***	4.8e-5 ***
L4 →L3	2.6e-2	7.3e-2	2.0e-2	4.1e-2	1.0e-3 *	1.4e-2

B. Individual Vertebrae Positions and Orientations Variability

The inter-vertebral poses variability model illustrated in Fig. 3 showed that the main rotational variability was found on the anterior-posterior axis. This was expected since orthopaedists routinely use the anterior-posterior radiograph to compute the Cobb angle (which is used to estimate scoliosis severity). Furthermore, the main translational variability was found in the axial direction which makes sense since the elongation of the spine that characterizes the growth process could be described using axial translations.

It was also noted that the relative contributions of the translational variability in the coronal direction and of the rotational variability in the sagittal direction are larger when absolute positions and orientations are considered. This greater variability along the natural flexion/extension motion axis of the spine tend to confirm that absolute positions and orientations are more suitable to analyse posture and motion, while relative positions and orientations are more adapted to the analysis of the anatomical variability.

Furthermore, there is also a significant proportion of the variability along all the degrees of freedom (DOF) of the inter-vertebral transforms. Thus, all the six DOF of the rigid transforms are needed to capture the variability of the spine shape. Practical implications of this improved knowledge of the variability include the design of new orthopaedic treatments (either braces or surgical instrumentations) that achieve a better balance between geometric correction and patient freedom of motion.

The representation of the spine shape as an articulated object is intuitive and the obtained results proved that anatomical insights can be gained that way. The Riemannian framework that was used to build the variability model naturally leads to the use of the rotation and of translation vector in the computation of the mean shape and of its variability. This representation was one of the keys to an intuitive visualization of both the mean spine shape and the variability around that

mean shape.

C. Effect of Orthopaedic Treatments

A visual comparison between the variability models associated with group II, III and IV (see Figs. 6, 5 and 7) revealed that the mean spine shape of treated patients seems closer to a healthy spine shape than the untreated patients. Furthermore, the variability of the spine shape deformations linked to a treatment appeared to be greater than the one linked to the progression of the disease. The variability associated with the Boston brace also appeared to be smaller than the variability associated with the Cotrel-Dubousset instrumentation.

More interestingly, the difference between the mean shape and the difference between the variability are not uniform. Table I clearly states that the Boston brace has a significant effect on the mean shape and on the variability for two different regions of the spine, respectively from T1 to T6 and from T8 to T12. This suggest a systematic effect of the Boston brace on the geometry of the upper-thoracic spine of all patients treated with it regardless of strength and shape of the curvature caused by scoliosis. It also suggest that severe scoliotic cases were submitted to larger corrections in the lower-thoracic segment of the spine than mild cases which lead to larger variabilities. Therefore, this difference suggests that most of the therapeutic effect of the Boston brace is localized in the region from T8 to L1. The effect of the Cotrel-Dubousset appeared to have a very sparse effect on the mean shape. However it has a significant effect on the variability associated with all the inter-vertebral transforms. This greater variability might explains the sparsity of the significant results obtained on the mean shape since a greater variability generally results in a reduction of the statistical power of tests performed on the mean. These results strongly indicate that not only the mean shapes but also the shape variabilities have to be analysed when two groups of patients are compared.

The Table II as a whole suggests that a surgical correction of scoliosis using a Cotrel-Dubousset instrumentation deforms

the spine towards a more “normal” spine shape, while the Boston brace has only a small effect on the distance to normality. This situation is understandable since a surgical intervention aims at correcting the deformity while a brace primarily goal is to stop the evolution of the deformity by applying subtle structural modifications.

Unfortunately, few of the distance differences associated with individual inter-vertebral level were found to be significant. A larger patient sample would be necessary to draw stronger conclusions from an analysis of these distances. The statistical tests performed directly on the centrality and dispersion measures (presented at Table I) seemed to be more powerful with the number of patients available and did not require a sample of healthy patients.

Moreover, surgical correction objectives are to optimally correct the spine deformity to obtain a spinal shape as “normal” as possible while instrumenting and fusing the least amount of vertebrae and avoiding complications. These contradictory objectives lead to a large variability among the spinal instrumentation configurations used by experienced surgeons [42]. Furthermore, what orthopedists usually defines as “normal” is not based on a statistical model of the spine geometry but on their clinical experience. More specifically, orthopedists usually try to obtain a straight spine in the frontal view with level shoulders and the trunk centered over the pelvis, a thoracic kyphosis between 20 and 40 degrees and a lumbar lordosis between 30 and 50 degrees in the sagittal view. The distance measure used to create the Table II approximate the correction objectives but do not take into account factors that are extrinsic to the spine geometry (shoulders and pelvis position, post-operative mobility, instrumentation strategies, *etc.*). Thus, the Table II is an indication that the proposed variability model can efficiently capture the geometric component of orthopedic correction of scoliosis, but the distance used to create it should not be used to clinically evaluate treatment outcomes.

In the context of the comparison of two corrective instrumentation of scoliosis, Petit et al. [14] published a comparison between modifications of the centers of rotations. Their results are compatible with ours although centers of rotation are not explicitly used here. However, only the means were compared in the study of Petit et al., while it is now clear that the variability should also be analyzed in this context.

V. CONCLUSION

A method to quantitatively analyze the variability of the spine shape was presented in this paper. The proposed method is based on the decomposition of the subjects’ spine shape into instances of an articulated shape model. This articulated shape model uses rigid transformations to describe the state of the link between each vertebra. Then, the use of a Riemannian framework enabled us to compute relevant statistics from this articulated shape model. In addition to the spine shape, a model to analyze and compare the effects of orthopaedic treatments on the spine geometry was also proposed and a visualization method of the variability models was developed as well. Finally, a comprehensive study of the scoliotic spine

shape variability and of the treatment effect variability for two well established treatments of scoliosis were presented (the Cotrel-Dubousset surgical instrumentation and the Boston brace).

Experimental findings included the observation that the variabilities of inter-vertebral transformations were inhomogeneous (lumbar vertebrae were more variable than for the thoracic ones) and anisotropic (with maximal rotational variability around the anterior-posterior axis and maximal translational variability in the axial direction). Furthermore, brace and surgery were found to have a significant effect on the Fréchet mean and on the generalized covariance. These significant differences were observed in specific regions of the spine where the treatments actually modified the spine geometry. The therapeutic effects of orthopaedic treatments could thus be precisely localized.

In this study the correlations between the motions of non-adjacent vertebrae were not analyzed. In that context, one of the future directions for our work will be to study the global motions of the spine using joint covariances. Moreover, it would be interesting to see if a global model could be linked to clinically used surgical classifications of the deformities or if one could use a global model to study curve progression.

The proposed method is not limited to the spine and could easily be extended to other bony structures (elbows, knees or fingers for instance). Moreover, the variability model could be used to constraint a deformation field like Little et al. [43] did or to incorporate statistics in the registration process as it was recently proposed by Commowick et al. [44].

In conclusion, this study suggests that medically relevant knowledge about the spine shape and its deformations can be obtained by studying articulated shape models. From an orthopaedist’s point of view, these findings could be used to optimize treatment strategies and diagnostic methods. For example, better braces (or surgical instrumentations) could be designed by exploiting the strong anatomical variability in the coronal plane and the localisation of their effects on the spine geometry could be analyzed more easily.

APPENDIX

A Riemannian manifold \mathcal{M} is a manifold possessing a metric that can be expressed as a smoothly varying inner product $\langle \cdot | \cdot \rangle_x$ in the tangent spaces $T_x \mathcal{M}$ for all points $x \in \mathcal{M}$. A local representation of this Riemannian metric is given by the positive definite matrix $G(x) = [g_{ij}(x)]$ when the inner product between two vectors v and w of the tangent space $T_x \mathcal{M}$ is written as $\langle v | w \rangle_x = v^T \cdot G(x) \cdot w$. The norm of a vector $v \in T_x \mathcal{M}$ is given by $\|v\| = \sqrt{\langle v | v \rangle}$ and the length of any smooth curve $\gamma(t)$ on \mathcal{M} can then be computed by integrating the norm of the tangent vector $\dot{\gamma}(t)$ along the curve:

$$L(\gamma) = \int_{t_1}^{t_2} \|\dot{\gamma}\| dt = \int_{t_1}^{t_2} \sqrt{\langle \dot{\gamma}(t) | \dot{\gamma}(t) \rangle} dt \quad (12)$$

In order to compute the distance between two points (say x_1 and x_2) of a connected Riemannian manifold, we have to take the minimum length computed among all the smooth

curves starting from x_1 and ending at x_2 . Thus, the distance $d(x_1, x_2)$ between those two points is:

$$d(x_1, x_2) = \arg \min_{\gamma} L(\gamma) \quad (13)$$

where $\gamma(0) = x_1$ and $\gamma(1) = x_2$.

The distance minimising curves γ between any two points of the manifold are called geodesics. Calculus of variations shows that the geodesics are the curves satisfying the following differential system (using Einstein summation convention).

$$\ddot{\gamma} + \Gamma_{jk}^i \dot{\gamma}^j \dot{\gamma}^k = 0 \quad (14)$$

$$\Gamma_{jk}^i = \frac{1}{2} g^{im} \left(\frac{\partial}{\partial x_k} g_{mj} + \frac{\partial}{\partial x_j} g_{mk} - \frac{\partial}{\partial x_m} g_{jk} \right) \quad (15)$$

Where Γ_{jk}^i are the Christoffel symbols and $[g^{ij}(x)]$ is the inverse of the local representation of the metric $[g_{ij}(x)]$.

Geodesic curves are unique in the sense that there is one and only one geodesic $\gamma_{x,v}$ starting from $x \in \mathcal{M}$ with a tangent vector $v \in T_x \mathcal{M}$ at $t = 0$. Using the geodesics, it is possible to define a diffeomorphism between a neighbourhood of $0 \in T_x \mathcal{M}$ and $x \in \mathcal{M}$ called the exponential map.

The exponential map at $x \in \mathcal{M}$ maps each vector v of the tangent plane $T_x \mathcal{M}$ to the point of the manifold reached by following the geodesic $\gamma_{x,v}$ in a unit time. In other words, if we have $\gamma_{(x,v)}(1) = y$, then $\text{Exp}_x(v) = y$. The inverse mapping is noted $\text{Log}_x(y) = v$. Moreover the distance with respect to the deployment point is simply given by the norm of the result of the logarithmic map (which is also the norm of the tangent vector in $T_x \mathcal{M}$). Thus:

$$\text{dist}(x, y) = \|\text{Log}_x(y)\| \quad (16)$$

The Exp_x and Log_x maps can be thought as the folding and unfolding operations that connect the tangent space at x and the manifold.

REFERENCES

- [1] V. Vijvermans, G. Fabry, and J. Nijs, "Factors determining the final outcome of treatment of idiopathic scoliosis with the boston brace: a longitudinal study." *J. Pediatr. Orthop. B*, vol. 13, pp. 143–149, 2004.
- [2] S. Delorme, H. Labelle, B. Poitras, C. H. Rivard, C. Coillard, and J. Dansereau, "Pre-, intra-, and postoperative three-dimensional evaluation of adolescent idiopathic scoliosis." *J. Spinal Disord.*, vol. 13, 2000.
- [3] S. Delorme, H. Labelle, C. E. Aubin, J. A. de Guise, C. H. Rivard, B. Poitras, C. Coillard, and J. Dansereau, "Intraoperative comparison of two instrumentation techniques for the correction of adolescent idiopathic scoliosis. rod rotation and translation." *Spine*, vol. 24, pp. 2011–2011, Oct 1999.
- [4] P. Papin, H. Labelle, S. Delorme, C. E. Aubin, J. A. de Guise, and J. Dansereau, "Long-term three-dimensional changes of the spine after posterior spinal instrumentation and fusion in adolescent idiopathic scoliosis." *Eur. Spine J.*, vol. 8, pp. 16–16, 1999.
- [5] L. G. Lenke, R. R. Betz, J. Harms, K. H. Bridwell, D. H. Clements, T. G. Lowe, and K. Blanke, "Adolescent idiopathic scoliosis: a new classification to determine extent of spinal arthrodesis." *J. Bone Joint Surg. Am.*, vol. 83-A, pp. 1169–1181, Aug 2001.
- [6] M. Ogon, K. Giesinger, H. Behensky, C. Wimmer, M. Nogler, C. M. Bach, and M. Krismer, "Interobserver and intraobserver reliability of lenke's new scoliosis classification system." *Spine*, vol. 27, pp. 858–862, Apr 2002.
- [7] C. T. Price, "The value of the system of king et al. for the classification of idiopathic thoracic scoliosis." *J. Bone Joint Surg. Am.*, vol. 81, pp. 743–744, May 1999.
- [8] I. A. F. Stokes and D. D. Aronsson, "Rule-based algorithm for automated king-type classification of idiopathic scoliosis." *Stud. Health Technol. Inform.*, vol. 88, pp. 149–152, 2002.
- [9] S. Delorme, H. Labelle, C. E. Aubin, J. A. de Guise, C. H. Rivard, B. Poitras, and J. Dansereau, "A three-dimensional radiographic comparison of cotrel-dubousset and colorado instrumentations for the correction of idiopathic scoliosis." *Spine*, vol. 25, pp. 205–210, Jan 2000.
- [10] J. R. Cobb, "Outline for the study of scoliosis." *Amer. Acad. Orthop. Surg. Instruct. Lect.*, vol. 5, 1948.
- [11] I. A. Stokes, "Three-dimensional terminology of spinal deformity. a report presented to the scoliosis research society by the scoliosis research society working group on 3-d terminology of spinal deformity." *Spine*, vol. 19, pp. 236–248, Jan 1994.
- [12] I. B. Ghanem, F. Hagnere, et al., "Intraoperative optoelectronic analysis of three-dimensional vertebral displacement after cotrel-dubousset rod rotation. a preliminary report." *Spine*, vol. 22, pp. 1913–21, 1997.
- [13] Sawatzky, Jang, Tredwell, Black, Reilly, and Booth, "Intra-operative analysis of scoliosis surgery in 3-d." *Comp. Meth. Biomech. Biomed. Eng.*, vol. 1, 1998.
- [14] Y. Petit, C.-E. Aubin, and H. Labelle, "Spinal shape changes resulting from scoliotic spine surgical instrumentation expressed as intervertebral rotations and centers of rotation." *J Biomech*, vol. 37, pp. 173–180, 2004.
- [15] T. Yrjonen, M. Ylikoski, D. Schlenzka, R. Kinnunen, and M. Poussa, "Effectiveness of the providence nighttime bracing in adolescent idiopathic scoliosis: a comparative study of 36 female patients." *Eur. Spine J.*, Jan 2006.
- [16] E. L. Laurnen, J. W. Tupper, and M. P. Mullen, "The boston brace in thoracic scoliosis. a preliminary report." *Spine*, vol. 8, pp. 388–395, 1982.
- [17] A. Uden and S. Willner, "The effect of lumbar flexion and boston thoracic brace on the curves in idiopathic scoliosis." *Spine*, vol. 8, pp. 846–850, 1983.
- [18] H. Labelle, J. Dansereau, C. Bellefleur, and B. Poitras, "Three-dimensional effect of the boston brace on the thoracic spine and rib cage." *Spine*, vol. 21, pp. 59–59, Jan 1996.
- [19] X. Pennec, "Probabilities and statistics on riemannian manifolds: basic tools for geometric measurements," *Proceedings of the IEEE-EURASIP Workshop on Nonlinear Signal and Image Processing (NSIP'99)*, vol. 1, pp. 194 – 8, 1999.
- [20] —, "Intrinsic statistics on Riemannian manifolds: Basic tools for geometric measurements," *Journal of Mathematical Imaging and Vision*, vol. 25, no. 1, pp. 127–154, 2006.
- [21] X. Pennec, P. Fillard, and N. Ayache, "A Riemannian framework for tensor computing," *Int. Journal of Computer Vision*, vol. 66, no. 1, pp. 41–66, 2006.
- [22] P. G. Batchelor, M. Moakher, D. Atkinson, F. Calamante, and A. Connelly, "A rigorous framework for diffusion tensor calculus," *Magn. Reson. Med.*, vol. 53, no. 1, pp. 221 – 225, 2005.
- [23] V. Arsigny, P. Fillard, X. Pennec, and N. Ayache, "Fast and simple calculus on tensors in the Log-Euclidean framework," in *Proc. of MICCAI*, ser. LNCS, vol. 3749, 2005, pp. 115–122.
- [24] C. Lenglet, M. Rousson, R. Deriche, and O. Faugeras, "Statistics on the manifold of multivariate normal distributions: Theory and application to diffusion tensor mri processing," *J. Math. Imaging Vis.*, 2005.
- [25] P. Fletcher and S. Joshi, "Principal geodesic analysis on symmetric spaces: statistics of diffusion tensors," *Proc. ECCV 2004 Workshops CVAMIA and MMBIA.*, pp. 87 – 98, 2004.
- [26] J. Boisvert, X. Pennec, N. Ayache, H. Labelle, and F. Cheriet, "3D anatomical variability assessment of the scoliotic spine using statistics on Lie groups," in *Proc. 2006 IEEE International Symposium on Biomedical Imaging*, 2006, pp. 750–753.
- [27] P. T. Fletcher, C. Lu, S. M. Pizer, and S. Joshi, "Principal geodesic analysis for the study of nonlinear statistics of shape," *IEEE Trans. Med. Imaging*, vol. 23, no. 8, 2004.
- [28] C.-E. Aubin, J. Dansereau, F. Parent, H. Labelle, and J. de Guise, "Morphometric evaluations of personalised 3d reconstructions and geometric models of the human spine," *Med. Bio. Eng. Comp.*, vol. 35, 1997.
- [29] X. Pennec and J.-P. Thirion, "A framework for uncertainty and validation of 3d registration methods based on points and frames," *Int. J. Comput. Vis.*, vol. 25, no. 3, pp. 203 – 29, 1997.
- [30] M. Fréchet, "Les éléments aléatoires de nature quelconque dans un espace distancié," *Ann. Inst. H. Poincaré*, vol. 10, pp. 215–310, 1948.

- [31] W. S. Kendall, "Probability, convexity, and harmonic maps with small image. i. uniqueness and fine existence." *Proc. London Math. Soc.*, vol. 3, no. 61, pp. 371–406, 1990.
- [32] D. Eggert, A. Lorusso, and R. Fisher, "Estimating 3-d rigid body transformations: A comparison of four major algorithms," *Machine Vision and Applications*, vol. 9, no. 5-6, pp. 272 – 290, 1997.
- [33] C. Gramkow, "On averaging rotations," *Int. J. of Computer Vision*, vol. 42, no. 1-2, pp. 7 – 16, 2001.
- [34] A. C. Rencher, *Methods of Multivariate Analysis*. Wiley, 2002.
- [35] W. J. Conover, *Practical Nonparametric Statistics*. Wiley, 1980.
- [36] D. G. Nel and C. A. Van Der Merwe, "A solution to the multivariate behrens-fischer problem," *Communications in statistics. Theory and methods*, vol. 15, no. 12, pp. 3719–3735, 1986.
- [37] T. Terriberry, S. Joshi, and G. Gerig, "Hypothesis testing with nonlinear shape models," *Proc. IPMI. Lecture Notes in Computer Science Vol. 3565*, pp. 15 – 26, 2005.
- [38] J. P. Shaffer, "Multiple hypothesis testing: A review," *Annual Review of Psychology*, vol. 46, pp. 561–584, 1995.
- [39] Y. Benjamini and Y. Hochberg, "Controlling the false discovery rate: a practical and powerful approach to multiple testing," *J. Roy. Statist. Soc. Ser. B*, vol. 57, no. 1, pp. 289–300, 1995.
- [40] R. L. Fernando, D. Nettleton, B. R. Southey, J. C. M. Dekkers, M. F. Rothschild, and M. Soller, "Controlling the proportion of false positives in multiple dependent tests," *Genetics*, vol. 166, pp. 611–619, Jan 2004.
- [41] M. O. Mosig, E. Lipkin, G. Khutoreskaya, E. Tchourzyna, M. Soller, and A. Friedmann, "A whole genome scan for quantitative trait loci affecting milk protein percentage in israeli-holstein cattle, by means of selective milk dna pooling in a daughter design, using an adjusted false discovery rate criterion," *Genetics*, vol. 157, pp. 1683–1698, Apr 2001.
- [42] C.-E. Aubin, H. Labelle, and O. C. Ciolofan, "Variability of spinal instrumentation configurations in adolescent idiopathic scoliosis," *Eur. Spine J.*, vol. 16, pp. 57–64, Jan 2007.
- [43] J. A. Little, D. L. G. Hill, and D. J. Hawkes, "Deformations incorporating rigid structures," *Computer Vision and Image Understanding*, vol. 66, no. 2, pp. 223–32, May 1997.
- [44] O. Commowick, R. Stefanescu, P. Pillard, P. Arsigny, N. Ayache, X. Pennec, and G. Malandain, "Incorporating statistical measures of anatomical variability in atlas-to-subject registration for conformal brain radiotherapy," *Proc. Med. Imag. Comp. and Comp.-Assist. Intervention*, pp. 927 – 34, 2005.